HIGHLY MESOPOROUS CARBONS OBTAINED USING A DYNAMIC TEMPLATE METHOD

Conchi O. Ania[@] and Teresa J. Bandosz*

Department of Chemistry, The City College of New York, New York, NY 10031, USA. E-mail: tbandosz@ccny.cuny.edu

[@] Present address: CRMD, CNRS, 1 rue de la Férollerie, 45000 Orléans, Cedex 2, France.

ABSTRACT

New nanoporous carbons with extremely high mesopore volumes and surface areas were obtained using mesoporous silica with a 3-D wormhole porous framework as templates. Mesoporous silica was synthesized following the literature described methods. Polystyrene sulfonic acid-based organic salts were used as carbon precursors. To evaluate the effect of sodium on porosity development silica matrices with various thicknesses of pore walls were synthesized. Prior to carbonization, in order to increase surface heterogeneity, the precursor chemistry was modified by cation exchange with catalytically active metals (i.e., copper, nickel, cobalt). Carbonization followed by HF etching of silica templates generated mesoporous carbons with large surface areas and high pore volumes, which is accompanied by high dispersion of catalytically active metals on the carbon surface. Sodium present in the carbonaceous precursor causes in the dynamic template effect via its reactions with a silica matrix during carbonization. This, along with reactive gases evolved during heating lead to the expansion of the carbonaceous structure, and thus to the unique wide mesopore size distributions of the templated carbons with pore sizes between 10 and 50 nm and their volume exceeding 2.5 $cm^3 g^{-1}$.

Keywords: Carbon; Dynamic template carbonization; Silica; Mesoporosity; Sodium effect

*corresponding author:
T.J. Bandosz, Chemistry Department of the City College of New York, 10031 New York, USA
Telephone: 01 (212) 650 6017 ; Fax: 01 (212) 650 6107; e-mail: tbandosz@ccny.cuny.edu

1. INTRODUCTION

Activated carbons have been extensively used in a large number of industrial applications, such as adsorption and separation processes. This is owing to their flexible coordination chemistry that allows an infinite possibility of 3-dimensional structures with expanded pore network, and to their ability to react with other atoms, such as oxygen or nitrogen, both on their surface and/or within the structural framework. In physical adsorption the size and volume of pores are important, thus microporous carbons are used for the sorption/separation of light gases, whereas carbons with broad pore sizes are applied for removal of toxins or other large organic molecules [1, 2].

Recent developments in technology require porous carbons with tailorable pore sizes, specific shapes of pores, and large surface areas. Preparation of such carbons has attracted widespread attention. This is the result of the demand for mesoporous materials in emergent areas such as energy storage (as double layer capacitors [3]), fuel cell catalytic supports [4], adsorption of bulky molecules form liquid phase [5], etc. Although to meet such demands many novel approaches to design a pore structure have been proposed [6] only a few of them allow for full control of porosity. The template carbonization has been proven to be an excellent method for obtaining carbons with large surface areas, high porosity and controlled narrow pore size distributions in the mesopore range [6]. Many polymeric precursors including polyacrylonitrile, poly(furfuryl alcohol), poly(vinylidene chloride), and phenol resin have been applied as porous carbon precursors [7-12].

In many applications the surface chemistry of carbons is of paramount importance. It determines the chemical stability and the reactivity in adsorptive and catalytic processes [2, 13]. A number of activated carbon applications have arisen because of the existence of a superficial layer of chemically bonded elements. The surface chemistry of activated carbon is the result of the presence of heteroatoms, usually coming from the precursor or activation agent. Very often, the natural chemistry of the activated carbon surface is not potent enough to enhance the specific adsorbate-adsorbent interactions or the catalytic properties of the carbon surfaces. Thus, the possibility of enhancing the physicochemical properties of carbons via modification of their

surface by the incorporation of the desired heteroatoms is among current research interests in the carbon science.

In the light of the above, mesoporous carbons synthesized in mesoporous silica templates attracted much attention as catalysts and adsorbents owing to their large pore dimensions compared to microporous adsorbents. However, despite their large pore dimensions, it is difficult to obtain mesoporous materials exhibiting specific catalytic and adsorption properties such as those characteristics of zeolites (i.e., uniform acidity). Some efforts have been made to obtain mesoporous materials endowed with a specific functionality [14-16], by means of generation of microporosity within the amorphous pore walls of mesoporous materials. However, performing that crystallization procedure in the thin walls of the mesopores materials is not an easy task.

Various methods have been described in the literature to modify carbon surface chemistry, [17-20]. One of them is pyrolysis of certain organic salts containing metal cations [21]. This method leads to carbonaceous materials with a high surface area and well-developed microporosity. Moreover, when the pyrolysis of polystyrene sulfonic acid-co-maleic acid salts is carried out at 1073 K, metal species are highly dispersed on the microporous carbon surface.

This work focuses on the development of highly mesoporous carbon materials using a dynamic carbonization-templating procedure. The objective of this research is to evaluate the combined effect of both sodium in the precursor and silica texture on the surface features of template-derived carbons. Moreover, the specific type of the carbon precursor used enables incorporation of highly dispersed catalytically active metals to the carbon matrix.

As templates, MSU-X silicas (X refers to the type of surfactant) are used. They are disordered mesoporous materials with a 3-D wormhole porous framework and pore sizes in the range of 2-50 nm [22]. Adjusting the conditions of the silica synthesis allows to tailor the thickness of their pore walls. A polystyrene-based polymer (poly-(styrene sulfonic acid co maleic acid)- sodium salt) is used as a carbon precursor. Prior to carbonization, in order to increase surface heterogeneity, the precursor chemistry is modified by cation exchange with catalytically active metals (i.e., copper, nickel, cobalt).

The originality of this work lays in the utilization of an organic sodium-containing salt that enables to obtain highly mesoporous carbons with large pore volumes, and the properties of the specific metals to modify surface chemistry and porosity of the final carbon. An important aspect of the preparation procedure is alteration of the surface properties by changing the contents of the metals. Thus, besides tailoring the porosity, the surface chemistry of the synthesized carbon can also be designed according to the desired application. The approach includes the synthesis of the mesoporous inorganic framework with different textural characteristics, the templating of the silica with carbon, and the characterization of the resulting materials after HF etching.

2. EXPERIMENTAL

Reagents. Poly(ethylene oxide)-PEO Tergitol 15-S-N, tetraethyl orthosilicate (TEOS, 98%), hydrochloric acid, sucrose (98%), cobalt (II) nitrate nickel (II) nitrate, and polystyrene-based polymer (poly-(styrene sulfonic acid co maleic acid)- sodium salt) were purchased from Sigma Aldrich. Copper (II) nitrate, NaF (99%) and HF (48%) were acquired from Fisher.

Synthesis of mesoporous silica. The mesoporous template was synthesized in a two-step pathway using tetraethyl orthosilicate as the silica source and a non-ionic surfactant following the procedure described by Boissiere et al. [23]. As a surfactant, non ionic poly(ethylene oxide) -PEO- surfactant Tergitol 15-S-N was selected. Briefly, the silica source (TEOS) was added under stirring to the solution of the non-ionic surfactant and the pH was adjusted at around 2 with HCl. The solution was kept in a closed vessel for 18 h without stirring at room temperature. Then a small amount of NaF was added to promote silica condensation. The final synthesis mixture composition followed the ratio TEOS:surfactant:NaF:HCl:H_2O = 1:0.125:0.06:0.064:375. The mixture was aged for 3 days at two temperatures, 303 K and 333 K. The white precipitate obtained was filtrated, dried and calcined at 873 K to eliminate the excess of the surfactant. The samples are referred to as T30 and T60, respectively.

Carbon templating. Sucrose and a polystyrene-based polymer (poly-(styrene sulfonic acid co maleic acid)- sodium salt) were used as carbon precursors in the template carbonization method.

For the sucrose synthesis, organic phase was introduced into the silica channels by liquids impregnation of a sucrose solution according to the process described by Ryoo et al. [24]. Briefly, the silica was impregnated with an aqueous solution of an organic precursor. After drying at 433 K, the organic precursor/silica composite is again impregnated with a sucrose solution and heated at 1073 K in an inert atmosphere. After two impregnation cycles, the amount of carbon deposited in the template represents 36 wt.%. In the case of polystyrene-based carbons, the silica was coated with an aqueous solution containing 16% of the organic salt, until the incipient wetness was achieved. The impregnated sample was then carbonized under nitrogen at 1073 K for 40 min. In some cases, the precursor chemistry was modified by incorporation of catalytically active metals. Previous to impregnation, cation-exchange in the organic precursor was done using $Cu(NO_3)_2$, $Co(NO_3)_2$, and $Ni(NO_3)_2$) as sources of cations. The exchanged polymer solutions were used to impregnate the silica matrix up to the incipient wetness. After removal of the silica matrix using hydrofluoric acid (48%) at room temperature, a Soxhlet washing with distilled water was carried out to remove an excess of water-soluble inorganic salts (sodium and excess of transition metal salts). The samples are referred to as T30 or T60 followed by SUC or PS M which stand either for sucrose or polymeric salt of a corresponding metal (T30-SUC or T60-PS Ni).

Characterization methods

Nitrogen adsorption

Textural characterization was carried out by measuring the N_2 adsorption isotherms at 77K. Before the experiments, the samples were outgassed under vacuum at 383 K. The isotherms were used to calculate the specific surface area, S_{BET}, total pore volume $p/p_o<0.99$), V_T, micropore volume, V_{mic}, mesopores volume, V_{mes}, and pore size distributions. The pore size distributions (micro and mesoporosity) were evaluated using density functional theory (DFT) [25].

XRD

X-ray diffraction (XRD) patterns at small (2θ = 0.5–5) angles were obtained on a Siemens D5000 instrument operating at 40 kV and 20 mA and using Cu K_α radiation (k = 0.15406 nm). The analyzed powdered carbon samples were spread as thin layers on a glass slide and analyzed.

SEM/TEM

The structure of the silica and carbon materials was characterized using a Ziess DSM 942 scanning electron microscope. The carbon particles were dispersed on a graphite adhesive tab placed on an aluminium stub. The images were generated using the backscattered electron signal, which yielded better quality pictures, but in some occasions, where a higher resolution was required, the settings were changed to the secondary electron mode. In any case, the information obtained was always topographic. The microtexture characterization of the templated carbons was realized by high-resolution transmission electron microscopy using a Philips CM20 working at 200 kV. For the analysis, a few milligrams of the sample were dispersed in anhydrous alcohol, and a droplet was put on a TEM grid covered by a lacey amorphous carbon.

3. RESULTS AND DISCUSSION

A disordered mesoporous silica material (MSU-1) which is known of its a 3-D wormhole structure was selected as a templates since it is known that by adjusting the conditions of the synthesis, it is possible to tailor the thickness of its pore walls (and porosity) [22]. This is a key factor to prove the dynamic effect of sodium from the carbon precursor on the development of porosity of template-derived carbons. XRD patterns of the silica samples obtained at different synthesis temperatures (i.e. 303 and 333 K) are collected in Figure 1. Both samples exhibit a single XRD peak, which is distinctive for this kind of silica materials [22]. The peak is shifted to lower angles as the synthesis temperature increases. Since MSU-1 silicas do not have an ordered structure, the single, broad peak in the XRD pattern reflects the pore-pore correlation distance. Thus, the silica wall thickness value can be calculated by subtracting the pore diameter value from d-spacing. As expected, the silica walls thickness decreased as a function of the synthesis temperature [23], varying from 1.5 nm at 303 K to 1.1 nm at 333 K (Table 1). These differences are important to evaluate the effect of sodium on the development of porosity in the final product. The TEM images of the samples confirmed that the synthesized silica exhibited the worm-hole porous framework (Figure 2. inset).

SEM micrographs collected in Figure 2 reveal the presence of particle aggregates of spherical shape within the micrometric range (2-10 micron). Details of the porous structure of the silica

samples are provided from the nitrogen adsorption isotherms. The structural parameters of the calcined silicas are listed in Table 1. Two different aging temperatures used for the synthesis of the silica lead to the development of mesostructured frameworks with different porous networks [27, 28]. Raising the aging temperature of the second step in the silica synthesis results in an increase in the pore diameter. This is expected taking into account the changes in the amphiphilic character of the surfactant with an increase in the temperature and the fact that the silica synthesis proceeds via an assembly mechanism between the organic surfactants and the silica source [29]. Both silica samples have mesopores of uniform sizes (Figure 3). The maximum of the pore size distributions for the T30 and T60 samples are in 2.7 nm and 3.7 nm, respectively. Moreover, the pore size distributions are narrow in both cases with a full width at the half maximum FWHM about ~1 nm. The results obtained are in good agreement with those reported by Alvarez et al. [28]. The BET surface areas decrease with an increase in hydrothermal temperature from 1014 to 980 m^2g^{-1} for T30 and T60, respectively.

It is important to use carbon precursor with a high carbon yield (atomic ratio of carbon after / before pyrolysis 40–50%) to limit the shrinkage induced by densification and preserve the overall shape of the structure. Despite the fact that sucrose does not have a high carbon yield (25%), it was selected for this study because it is water soluble and thus easy to handle. In the case of the polystyrene sulfonic acid –based salts, the yield after carbonization represents approximately 40%, although it decreases significantly after water and acid washing due to the removal of water-soluble salts, sulfates and oxides [21]. Nevertheless, this precursor allows the possibility of metal incorporation to the carbonaceous matrix of the templated carbon.

The morphology of the silica particles and their structural characteristics are preserved in the templated carbons, as presented in SEM images in Figure 4. The carbon replicas, like the MSU-1 parent silica, are made up of spherical particles with diameters of 2-10 μm, regardless the carbon precursor. However, as opposite to nickel and cobalt, for the sample obtained from the copper-containing polystyrene-based carbon precursor, along with the carbon spheres, a bunch of metallic clusters appeared randomly dispersed on the surface of the carbon matrix. SEM micrographs show numerous particle aggregates of metal of a few nm in size. Taking into account the low reduction potential of the pair Cu(II)/Cu (+ 0.34 V), and the reductive

atmosphere during carbonization, the chemical status of copper in these aggregates is assigned to copper zero. It seems reasonable to think that during carbonization formation of metallic particle occurs, and the aggregates are produced as a result of migration of the reduced metals to the surface [21, 30]. This metallic copper is not oxidized by H^+ coming from acid during the washing step, thus it stays on the external surface of the spheres. Moreover, EDX analysis of the templated carbon particles showed that, despite the clusters, metals are also highly dispersed inside the carbon matrix and their particle sizes must be smaller than the resolution of our SEM images. Further observation of the copper-loaded sample by TEM (Fig. 5 d) corroborated the presence of the metallic aggregates of a few nm in size. The diffraction patterns presented in Figure 6 show well-dispersed metal sulfides, sulfur, and oxides agglomerates present on the surface of our materials. Similar results were obtained by Hines et al. when the same polymeric salts were used as carbon precursors [21].

The low angle range of the XRD patterns for the template-derived carbons are shown in Figure 1. The samples obtained from sucrose as a carbon precursor have a diffraction pattern similar to that of the MSU-1, with a broad peak in the low angle range, indicating the replication of the wormhole structure. On the other hand, application of a polystyrene-based salt as a carbon precursor leads to a strong alteration of the silica template. In all cases, the diffraction peak at the low angle range disappeared, indicating that the wormhole structure of the silica is not replicated and that the carbons posses a completely disorganized structure. This is not considered here as a failure since our goal was development of highly mesoporous carbons, not necessary with the wormhole structure of the silica.

The main textural characteristics of the templated carbons are collected in Table 2 in comparison with the data obtained for PS carbon obtained without any silica template [21]. Carbons prepared from sucrose have high surface areas up to 1500 m^2g^{-1}, and pore volumes up to 1 cm^3g^{-1}. These carbons also have micropore volumes of around 0.210 cm^3g^{-1}, which is likely related to the intrinsic microporosity of the carbon precursor. For both samples a capillary condensation occurs in the p/po range between 0.1- 0.4 and 0.3- 0.6 (Figure 7), which clearly indicates that the structural porosity of the silica framework is replicated in the carbon. The pore size distributions for these carbons are very narrow with FWHM 1.2 nm and 1 nm, for T30 SUC and T60 SUC,

respectively (Figure 8). Additionally, a slight development of complementary mesoporosity (estimated from the amount of nitrogen adsorbed at $p/p_o > 0.7$) can be seen, accounting for 6 % and 7 % of the total pore volume (Table 2). It is worth to mention that the pore size corresponding to the porosity that originated from the silica framework is around 3.2-3.4 nm, which is slightly different than the one measured for carbons prepared from furfuryl alcohol (around 3.0 nm) reported by Alvarez et al. [28]. This difference corroborates the hypothesis that depending on the type of carbon precursor used to infiltrate the silica porosity, it is possible to change the size of the mesopores derived from the silica framework [28].

Use of a polystyrene-based organic salt as a carbon precursor, as well as the incorporation of metals to the carbonaceous structure leads to highly porous materials, with notable differences in the porosity if compared with the sucrose-derived carbons. The replicated carbons are mesopore systems, as indicated by the presence of a large hysteresis loop and capillary condensation step at high relative pressures seen on the isotherms (Figure 7). All the samples show two capillary condensation steps at relative pressures between 0.2-0.4 and $p/p_o > 0.7$. The first one, as it also appears for the silica, is associated to the structural porosity – framework of confined mesopores- resulting from the dissolution of the inorganic template. The second condensation step at relative pressures > 0.7 is assigned to the porosity (complementary or textural porosity) that arises from either interparticle voids due to the agglomeration of very fine particles which contains framework-confined mesopores [31] or it is the effect of the reaction of sodium with the silica during carbonization which leads to destruction of thin pore walls and formation of large pores in the template. Since the latter effect is dynamic and occurs during carbonization the only feasible way to control it is by changing the thickness of pore walls and the content of sodium. As estimated from nitrogen adsorption, this complementary mesoporosity accounts for almost 80 % of the porosity in the samples templated from the T60 silica. Indeed, the pore walls in the parent silica are thinner in T60 than those in T30. For the samples obtained from T30, complementary mesoporosity represents between 65-75 % of the total porosity. An exception is for carbon obtained from cobalt salt for which the relatively small volume of large mesopores was formed (48 %). These differences might be due to the different amounts of precursors loaded to the silica matrix. The T60 besides having thinner pore walls has also the larger pore volume, which leads

to the higher amount of the carbon precursor then in T30, and thus, the contribution of complementary pores is larger.

Comparison of the textural parameters of the template-derived samples to those of the carbon obtained by direct carbonization reveals striking differences. Although as a result of the template carbonization approach the surface area and volume of micropores significantly decreased and its consists of only about 70% of the surface of the PS sample, the value of mesopores is exceptionally high (sixteen times more for T60PS in comparison with PS) with the total pore volume exceeding 3.5 cm^3/g. This is three times more than that of the direct carbonization counterpart. These striking differences have to be related to the combined effect of the silica template and chemistry of the precursor. Support for this is the dissimilar texture of sucrose-derived carbon where the matrix was the same but the precursor was chemically inert with respect to the matrix.

The presence of metallic cations in the carbon precursor and in the final structure of the template-derived carbons has an effect on the overall porosity of the samples. As indicated elsewhere [21], the functionalities of the carbon precursor play also a role in the development of porosity in the final materials. It happens due to the decomposition of sulfonic groups in H_2S followed by decomposition of sodium sulfide and migration of metals to the surface. This is seen by the relatively high degree of microporosity developed in the template-derived carbons (Table 2). Nevertheless this volume of micropores is twice less in comparison with the sample obtained using direct carbonization.

It is noteworthy that adsorbents obtained from nickel and copper salts have large surface areas and high volumes of mesopores (Table 2). Moreover, the close similarities in the pore size distributions exist, especially for the complementary mesopores. The PSDs presented in Figure 8 show wide distributions with a maximum at 20 nm. A remarkable difference in porosity is noticed for the cobalt-containing sample for which the peak related to the complementary mesopores (48 %) is much narrower (maximum at 9.3 nm) and has lower intensity than those for the nickel and copper counterparts. This is accompanied by the smaller BET surface area than those for copper, nickel, or sodium counterparts. This effect was not observed in the case of

carbonization of a cobalt-loaded precursor in the absence of template [21]. Since in the case of cobalt salt-derived carbons a unique cardboard like structure was found when the carbons were directly synthesized, it is possible that within the silica framework this “pseudo-organized” units could not be developed due to the space constrains. As a result of this the volume of mesopores is underdeveloped. It might happen only in small spaces and in fact the pores in T30 are smaller than those in T60. Support for this hypothesis is a high volume of mesopores, comparable for those for Cu and Ni-containing samples, in the PS Co sample obtained in T60 where the pores are considerably larger.

Direct analysis of the materials’ nanostructures using TEM (Figure 5) provide further information to explain the differences observed on the nitrogen adsorption isotherms. For the sample prepared from sucrose as a carbon precursor, the porous framework appears to be homogenous and characteristic of the 3D-wormhole porosity of the inorganic template, with a narrow mesoporosity well distributed within the sample. On the contrary, the analysis of the micrographs of the PS-templated carbons confirms the presence of wide mesopores. The worm-hole structure of silica is randomly present in these carbons indicating their completely disorganized structure. The differences in the porous structure between T30 PS and T60 PS are also seen from the micrographs (Figure 5). The complementary pores in T60 are slightly bigger than those on T30 as a result of its thinner pore walls of the silica matrix. The presence of metals/salts detected using EDX is revealed on TEM micrographs as spots of about 10 nm in diameter distributed evenly in the carbonaceous matrix (arrows in Figure 5).

The origin of the textural porosity in the template-derived carbon is complex. It was attributed in the literature to the water-vapor released during the carbonization process (due to the use of a liquid carbon precursor) that could hydrolyze the poorly hydrothermally stable silica network [32] and then be released as a pore former. In the case of our materials, the volume of complementary mesopores is relatively small when a sucrose solution is used as a precursor (10 % and 16 % for T30 suc and T60 suc, respectively). According to Fuertes and coworkers [33] the impregnation method affects the porous structure of the templates. They attributed the formation of complementary mesopores to the coalescence of unfilled silica pores during carbonization, and the subsequent collapse of the porous structure when silica walls are removed (thus, the sizes

of the mesopores increases remarkably). Following this hypothesis, the one-step infiltration procedure with the organic salt (as opposed to the 2 step impregnation procedure of the sucrose providing a better impregnation of the silica pores) should lead to a larger number of unfilled silica pores that coalescence during carbonization and collapse resulting in a broad distribution of mesopores.

It was found that using 2-steps impregnation, the porosity of the sample decreased (i.e. lower BET and pore volumes) and the PSD showed wider mesopores, instead of the expected narrower distribution suggested by Fuertes and coworkers [33]. This proves that even if the impregnation efficiency is enhanced by the second infiltration step, the role of sodium is definitively the crucial factor in the development of the mesoporosity. When more sodium is present within the silica the resulting carbons have a wider mesopores size distribution.

It is important to mention that in the case of our samples, another important factor associated with the composition of the carbon precursor contributes to porosity development. As mentioned above, during carbonization sodium salts react with the silica walls and erode them. Thin pore walls easily collapse as a result of the internal pressure caused by gases released during carbonization [21]. Moreover, internal silica matrix space constrains cause that local gas accumulation areas are formed creating large pores in the templated carbons. We refer to this process as *a dynamic template effect*. It is likely that the sizes of pores can be controlled by the amount of sodium in the polymer (erosion of walls) and the amount of released gases. The fact that for the thinner pore walls silica template (T60) and the same content of sodium in the polymer (after cation exchange sodium is also present in the system) the remarkably similar distributions of pore sizes are obtained, supports the hypothesis about the existence of this effect and its role for porosity development.

To determine the existence of the mentioned above effect of sodium on the structure of the silica matrix, one silica sample, T60, was infiltrated by the organic precursors (sucrose and PS), carbonized and washed as described in the experimental section. Then the carbon phase was removed by calcination of the silica-carbon composites in air at 1073 K. The recovered silicas (denoted as *b* followed by the carbon precursor) were characterized by nitrogen adsorption. For valid comparison, one non-infiltrated silica sample was heated at the same temperature, to consider the effect of the temperature on the inorganic framework (T60 H). The isotherms for

recovered T60 silica series are presented in Figure 3. The trend for T30 series is the same and therefore has not been included. As shown in Table 1, the cell parameter of the sucrose-templated burnt silica (T60 b suc) is close to the corresponding silica template. Compared to the initial silica sample, the sucrose-infiltrated one (T60 b suc) shows a small reduction in the pore volume (14 %) and BET surface area (23 %), which is due to the silica shrinkage during carbonization/ heat treatment [10]. This effect, however less pronounced is also observed for T60 H sample. On the other hand, in the case of the PS carbon precursor, the dramatic reduction in the BET surface area and pore volume clearly supports the dynamic template effect, and it cannot be attributed to the structural shrinkage of the silica as in the case of non-sodium containing precursor.

4. CONCLUSIONS

The results of this study show the feasibility of using a template carbonization method to obtain extremely mesoporous carbons with highly dispersed metals and spherical morphology . A disordered MSU-1 silica is used as a template and polystyrene-based organic salts as carbon precursors. The template-derived carbons have large pore volumes (up to 2.5 cm^3g^{-1}) in the mesopores/macropore range (10-100 nm), and highly dispersed catalytic metals on the surface. The presence of reactive gases during carbonization results in expansion of the carbonaceous structure, and thus in the broad mesopore size distributions. Another crucial factor for porosity development is sodium in the carbon precursor, which reacts with the silica during carbonization causing erosion of the pore walls. When exposed to internal pressure of gases released from the precursor these walls collapse. Allowing for further expansion of gases and formation of large pores.

These results constitute a novel route for engineering not only the texture, but also the surface chemistry (i.e., metal dispersion) of carbon materials for the intended application. The unique combination of large pore volumes, and highly dispersed metals in the carbon matrix make them useful for catalysis and for adsorption of large molecules, bacteria, or viruses. A high volume of large mesopores would be very useful for processes where rapid mass transfer steps take place

when large molecules are involved, such as supercapacitors and adsorption of non-aqueous electrolytes.

Acknowledgments

The financial support for this research, provided by FICYT and PSC CUNY (PSC CUNY 66382-0035) is gratefully acknowledged. We thank Dr. Pis and Dr. Beguin for kindly providing SEM and XRD, and TEM, respectively. Thomas Cacciaguerra is also acknowledged for assistance in TEM analysis.

REFERENCES

[1] F. Derbyshire, M. Jagtoyen, R. Andrews, A. Rao, I. Martín-Gullón, E.A. Grulke, (Eds. Radovic LR.) Chemistry and Physics of Carbon vol. 27, Marcel Dekker, New York, 2000, pp 1-66.

[2] C. Moreno-Castilla, Carbon 42 (2004) 83.

[3] S. Yoon, J. Lee, T.Hyeon, S.M. Oh, J. Electrochem. Soc. 147 (2000,) 2507.

[4] S.H. Joo, S.J. Choi, I.Oh, J.Kwak, Z.Liu, O.Teresaki, R. Ryoo, Nature 412 (2001) 169.

[5] S. Han, K. Sohn, K.; Hyeon, T. Chem. Mater. 12 (2000) 3337.

[6] T. Kyotani, Carbon 38 (2000) 269.

[7] S.B. Yoon, G.S. Chai, S.K.Kang, J.S.Yu, K.P. Gierszal, M. Jaroniec, J. Am. Chem. Soc. 127(2005) 4188.

[8] M. Kruk, B. Dufour, E. Celer, T.Kowalewski, M. Jaroniec, K.J. Matyjaszewski, J. Phys. Chem. B 109 (2005) 9216.

[9] L. Feng, S.H. Li, J. Zhai, Y.L. Song, L. Jiang, D.B. Zhu, Synthetic Metals 135-136 (2003) 817.

[10] A.B. Fuertes, Micro. Meso. Mater. 67 (2004) 273.

[11] C.J. Meyers, S.D. Shah, S.C. Patel, R.M. Sneeringer, C.A. Bessel, N.R. Dollahon, R.A. Leising, E.S. Takeuchi, J. Phys. Chem. B 105 (2001) 2143.

[12] T. Kyotani, T. Nagai, S. Inoue, A. Tomita, Chem. Mater. 9 (1997) 609.

[13] L.R. Radovic, C. Moreno-Castilla, J. Rivera-Utrilla, (Ed. Radovic LR) Chemistry and Physics of Carbon Vol. 27; M. Dekker, New York, 2000, pp 227-406.

[14] K.R. Kloetstra, H. Bekkum, J.C. van Jansen, Chem. Commun. (1997) 2281.

[15] P. Yang, D. Zhao, D.I. Margolese, B.F. Chmelka G.D. Stucky, Nature 396 (1998) 152.

[16] P. Yang, D. Zhao, D.I. Margolese, B.F. Chmelka G.D. Stucky, Chem. Mater., 11 (1999) 2813.

[17] H Oka, M. Inagaki, Y. Kaburagi, Y. Hishiyama, Solid State Ionic, 121 (1991) 157.

[18] F. Goutfer-Wurmser, H. Konno, Y. Kabuagi, K. Oshida, M. Inagaki, Synth. Met. 118 (2002) 33.

[19] M. Inagaki, Y. Okada, K. Miura, H. Konno, Carbon 37 (1999) 329.

[20] C. Zhou, J. Kong, E. Yenilmez, H. Dai, Science 290 (2000) 1552.

[21] D. Hines, A .Bagreev, T.J. Bandosz, Langmuir 20 (2004) 3388.

[22] S.A. Bagshaw, E. Pouzet, T.J. Pinnavaia, Science 269(1995) 1242.

[23] C. Boissiere, A. Larbot, A. van der Lee, P.J. Kooyman, E. Prouzet, Chem Mater., 12 (2000) 2902.

[24] R. Ryoo, S.H. Joo, S. Jun, J. Phys. Chem. B 103 (1999) 7743.

[25] J. Olivier, Carbon 36 (1998) 1469.

[26] T.J. Bandosz, M.J. Biggs, K.E. Gubbins, Y. Hattori, Y. Liyama, K. Kaneko, J. Pikunic, K.T. Thomson, (Ed. Radovic LR), Chemistry and Physics of Carbons vol. 28, Marcel-Dekker, New York, 2003, pp 41.

[27] E. Prouzet, T.J. Pinnavaia, Angew Chem Int Ed., 36 (1997) 516.

[28] S. Alvarez, A.B. Fuertes, Carbon 42 (2004) 423.

[29] C. oissiere, M.A.U. Martines, M. Tokumoto, A. Larbot E. Prouzet, Chem. Mater., 15 (2003) 509.

[30] H. Konno R. Matsumura, M. Yamasaki, H. Habazaki, Synth. Met. 1215 (2002) 167.

[31] A.B. Fuertes, Materials Letters, 58 (2004) 1494.

[32] J. Parmentier, C. Vix-Guterl, P. Gibot, M. Reda, M. Ilescu, J. Werckmann J. Patarin, Micro. Meso. Mater. 62 (2003) 87.

[33] A.B. Fuertes, D.M. Nevskaia, Micro. Meso. Mater. 62 (2003) 177.

CAPTIONS TO THE FIGURES

Figure 1.
XRD pattern for silica matrices and template derived carbons.

Figure 2.
SEM micrographs of calcined silicas at different magnifications (a: T30, b: T60) and TEM images of porous structure of the silicas (insets).

Figure 3.
Nitrogen adsorption isotherms (A) and PSDs (B) for silcas templates before and after removal of carbon.

Figure 4.
SEM micrographs of the template derived carbons: a) T60 SUC, b) T60 PS, c) T60 PS Cu, d) T60 PS Ni, e) T60 PS Co, (magnification is 5 micron, except when specified).

Figure 5.
TEM images of the porous structure of the templated carbon

Figure 6.
EDX patterns of the metal-loaded templated carbons (signals of the copper and nickel-containing samples have been vertically shifted for clarity).

Figure 7.
Nitrogen adsorption isotherms (at 77 K) for the carbons derived in T30 (A) and T60 (B) silicas.

Figure 8.
Pore size distributions for carbons derived in T30(A) and T60 (B) silicas obtained from nitrogen adsorption data.

CAPTIONS TO THE TABLES

Table 1.

Structural parameters of the calcined silica frameworks calculated from XRD and nitrogen adsorption data.

Table 2.

Structural parameters of template derived carbons, calculated from nitrogen adsorption isotherms

Table 1
Structural parameters of the silica frameworks calculated from XRD and nitrogen adsorption data

Silica	S_{BET} [m^2 g^{-1}]	V_T [cm^3 g^{-1}] p/p_o<0.99	d[a] [nm]	Wall thickness [nm)][b]	Pore size [c] [nm]
T30	1042	0.560	4.2	1.5	2.7
T60	989	0.903	4.8	1.1	3.7
T60 H	746	0.766	4.8	1.1	3.7
T60 b suc	692	0.529	4.7	1.3	3.4
T60 b PS	83	0.415	---	---	---

a Interplanar spacing
b Due to the disordered porous framework, wall thickness was calculated by subtracting the pore diameter from the *d* spacing.
c Average pore diameter at the maximum of the PSD evaluated from DFT.

Table 2
Structural parameters of template derived carbons, calculated from nitrogen adsorption isotherms

Sample	S_{BET} [m^2 g^{-1}]	V_{mic} [cm^3 g^{-1}] (DFT)	V_{mes} [cm^3 g^{-1}] (DFT)	V_T [cm^3 g^{-1}] p/p_o<0.99	V at p/p_o>0.7 [cm^3 g^{-1}]	Complementary Mesopores [%]
PS	1378	0.460	0.140	0.93	----	----
T30 PS	997	0.083	1.754	2.42	1.57	65
T30 PS Ni	959	0.131	2.171	2.60	1.846	71
T30 PS Cu	907	0.073	2.426	2.87	2.15	75
T30 PS Co	820	0.118	0.989	1.29	0.623	48
T30 SUC	1560	0.221	0.652	0.99	0.055	6
T60 PS	943	0.081	2.228	3.61	2.811	78
T60 PS Ni	758	0.087	1.869	2.25	1.661	74
T60 PS Cu	661	0.054	1.949	2.46	1.912	78
T60 PS Co	738	0.073	1.942	2.32	1.732	75
T60 SUC	1382	0.212	0.861	1.20	0.083	7

Fig. 1. XRD patterns of the inorganic framework and the templated carbons.

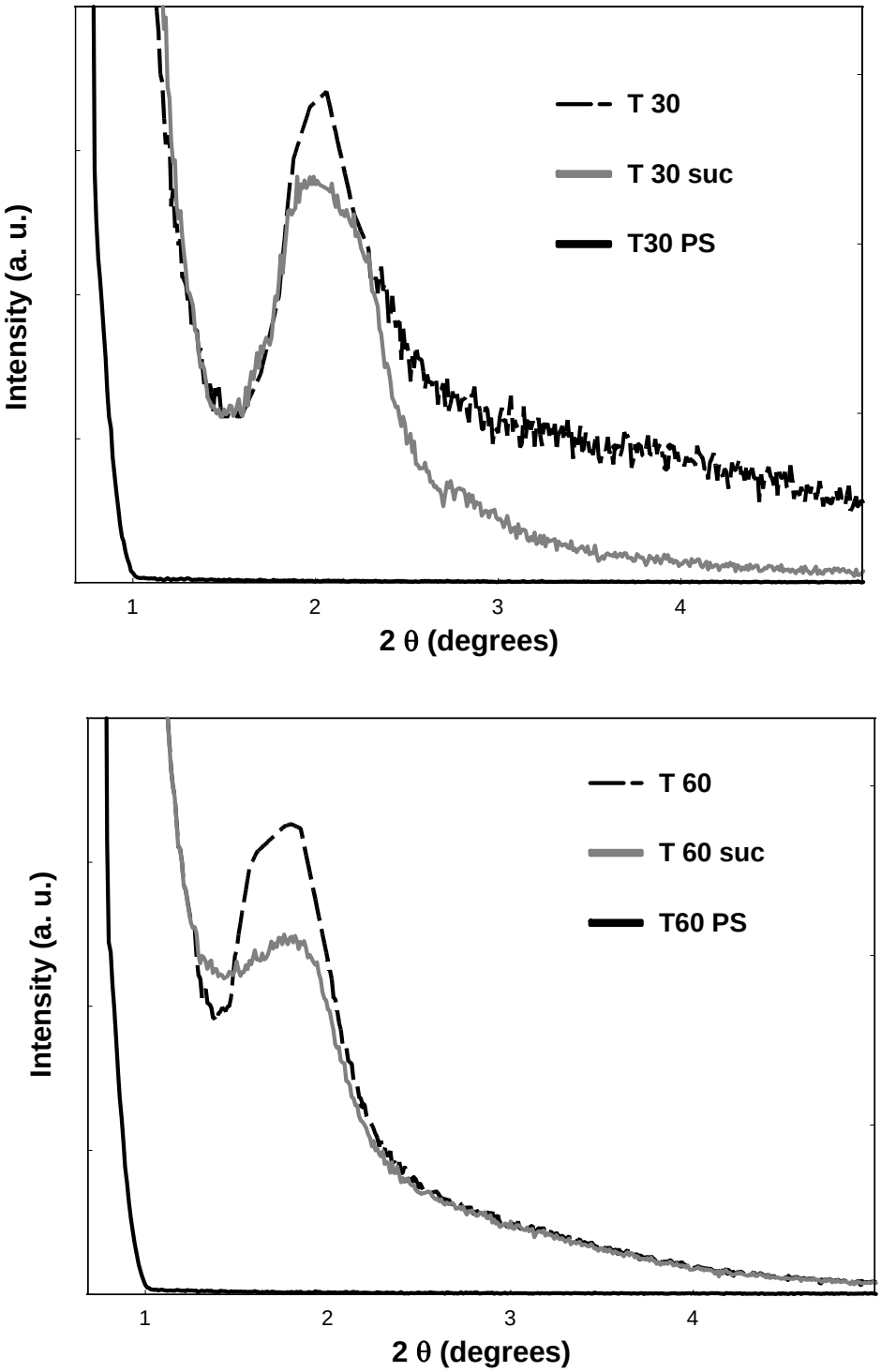

Fig. 2. SEM images of calcined silicas at different magnifications (A: T30, B: T60) and TEM images of porous structure of the silicas (inset).

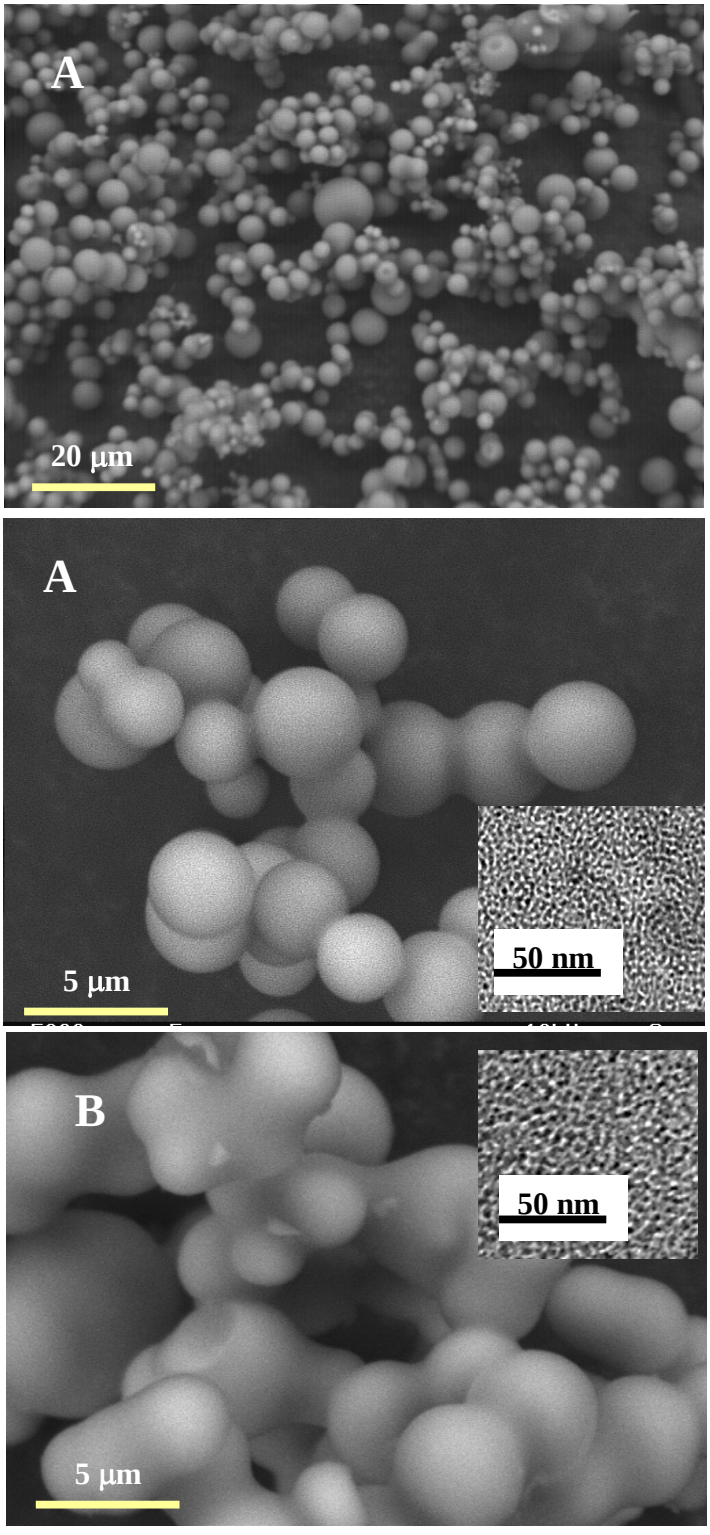

Figure 3. Nitrogen adsorption isotherms (A) and pore size distributions (B) of the original and recovered silica frameworks.

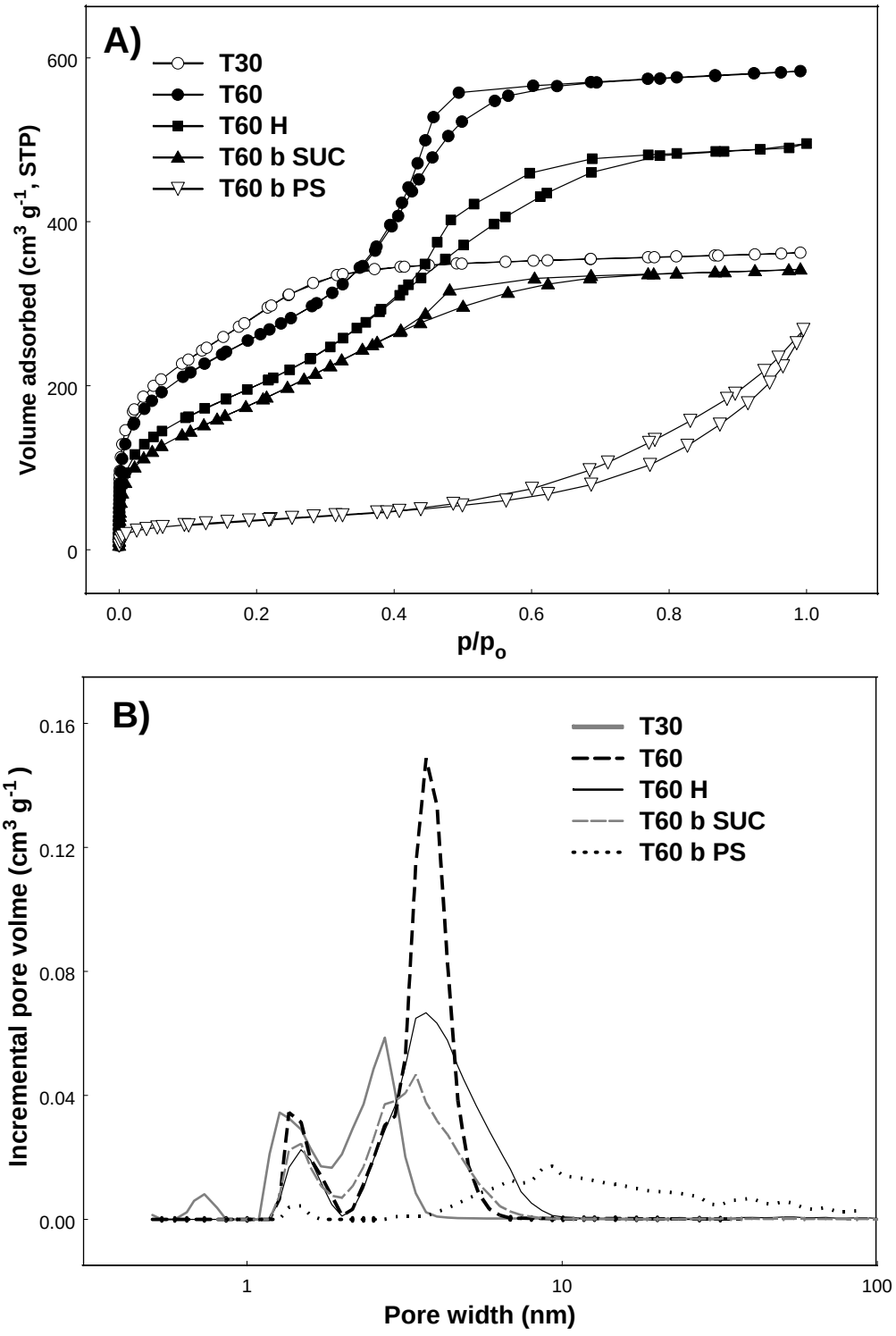

Fig. 4. SEM micrographs of the templated carbons: A) T60 SUC, B) T60 PS, D) T60 PS Cu, D) T60 PS Ni, E) T60 PS Co, (magnification is 5 micron, except when specified).

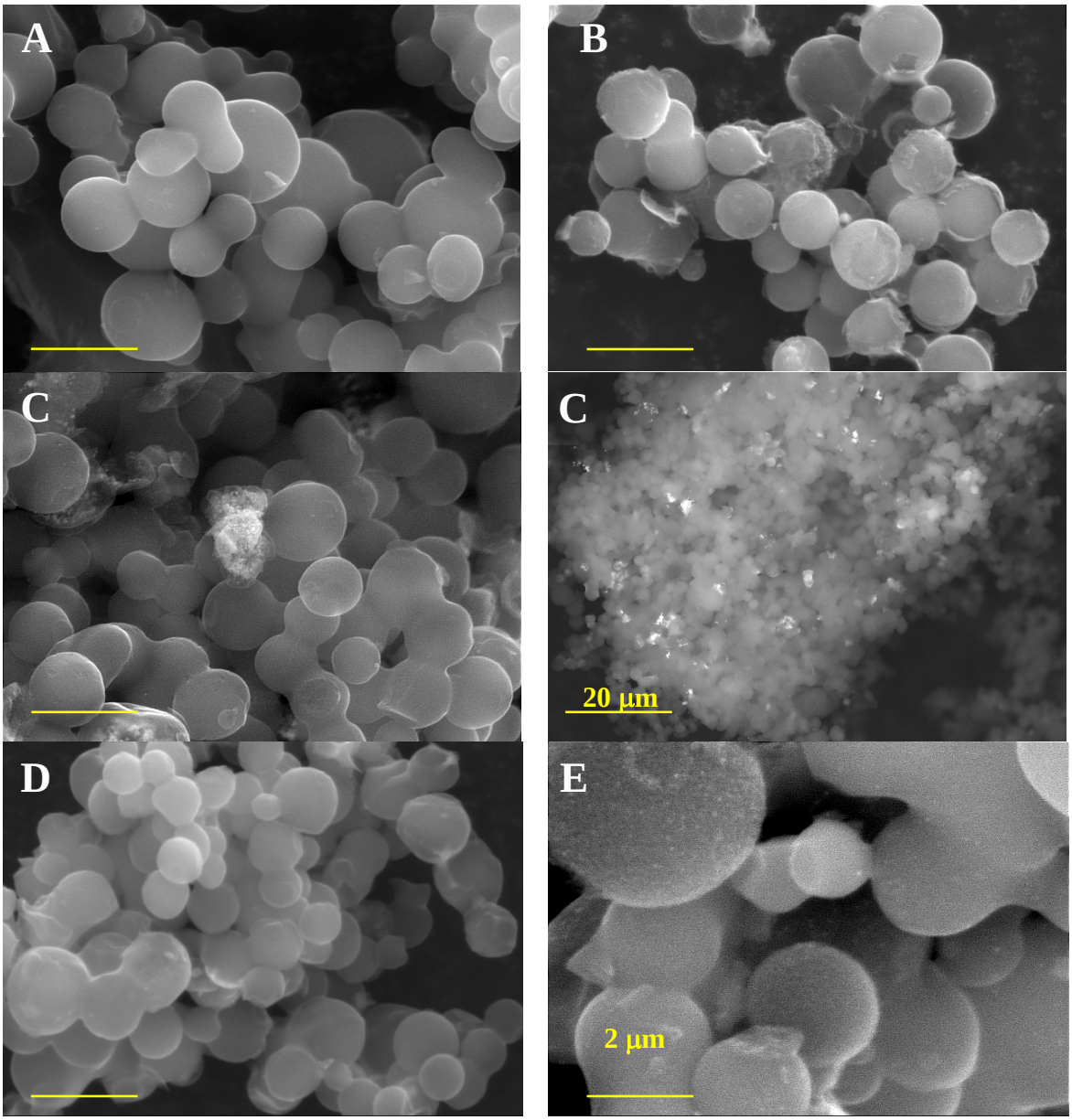

Figure 5. TEM images of the porous structure of the templated carbons.

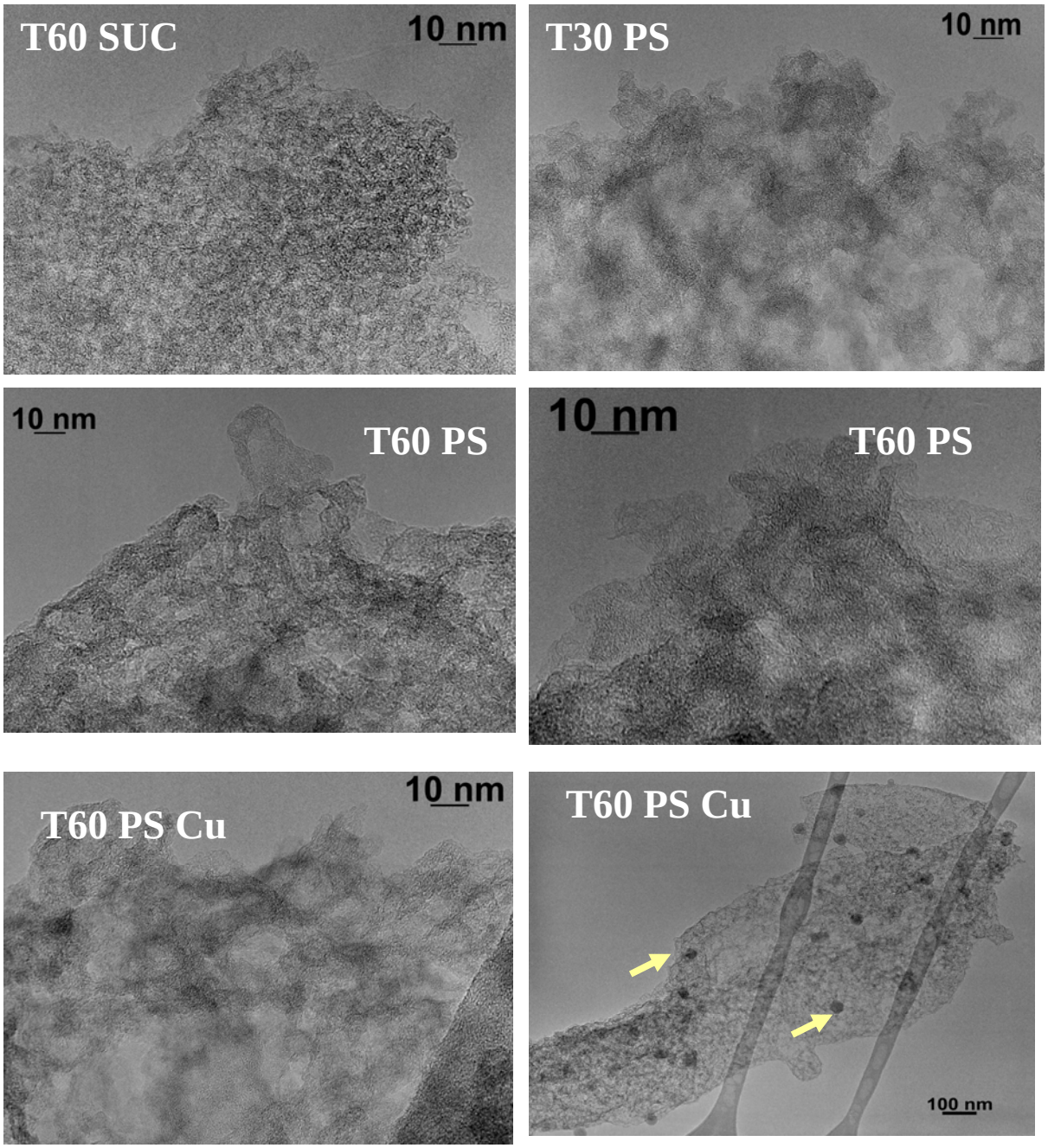

Fig. 6. EDX patterns of the metal-loaded templated carbons (signals of the copper and nickel-containing samples have been vertically shifted for clarity)

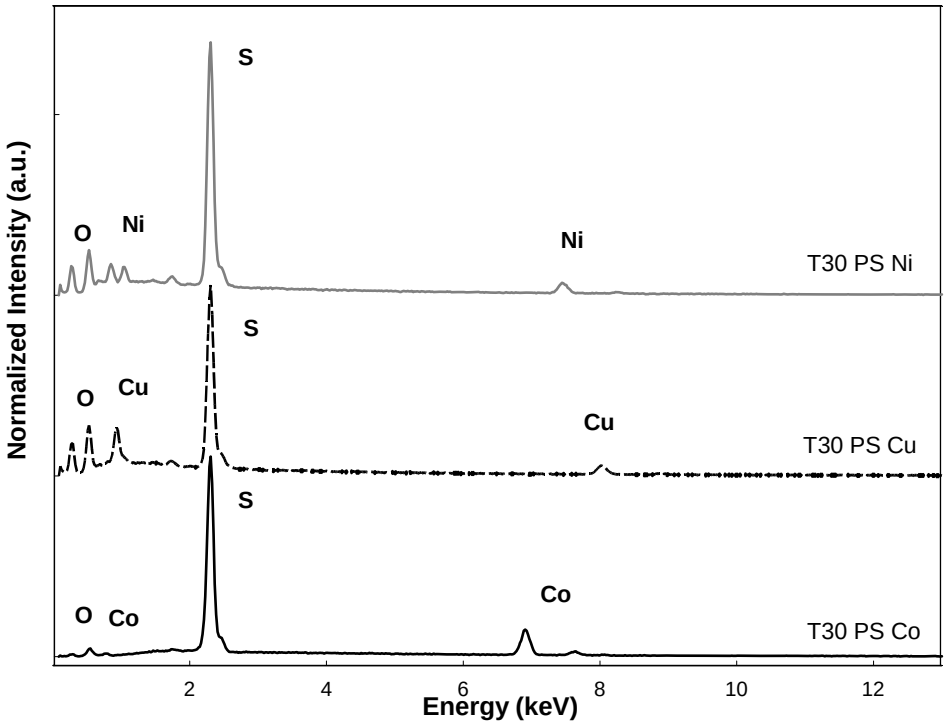

Fig. 7. Nitrogen adsorption isotherms at 77 K and PSD of the carbons derived in T30 (A) and T60 (B) silicas

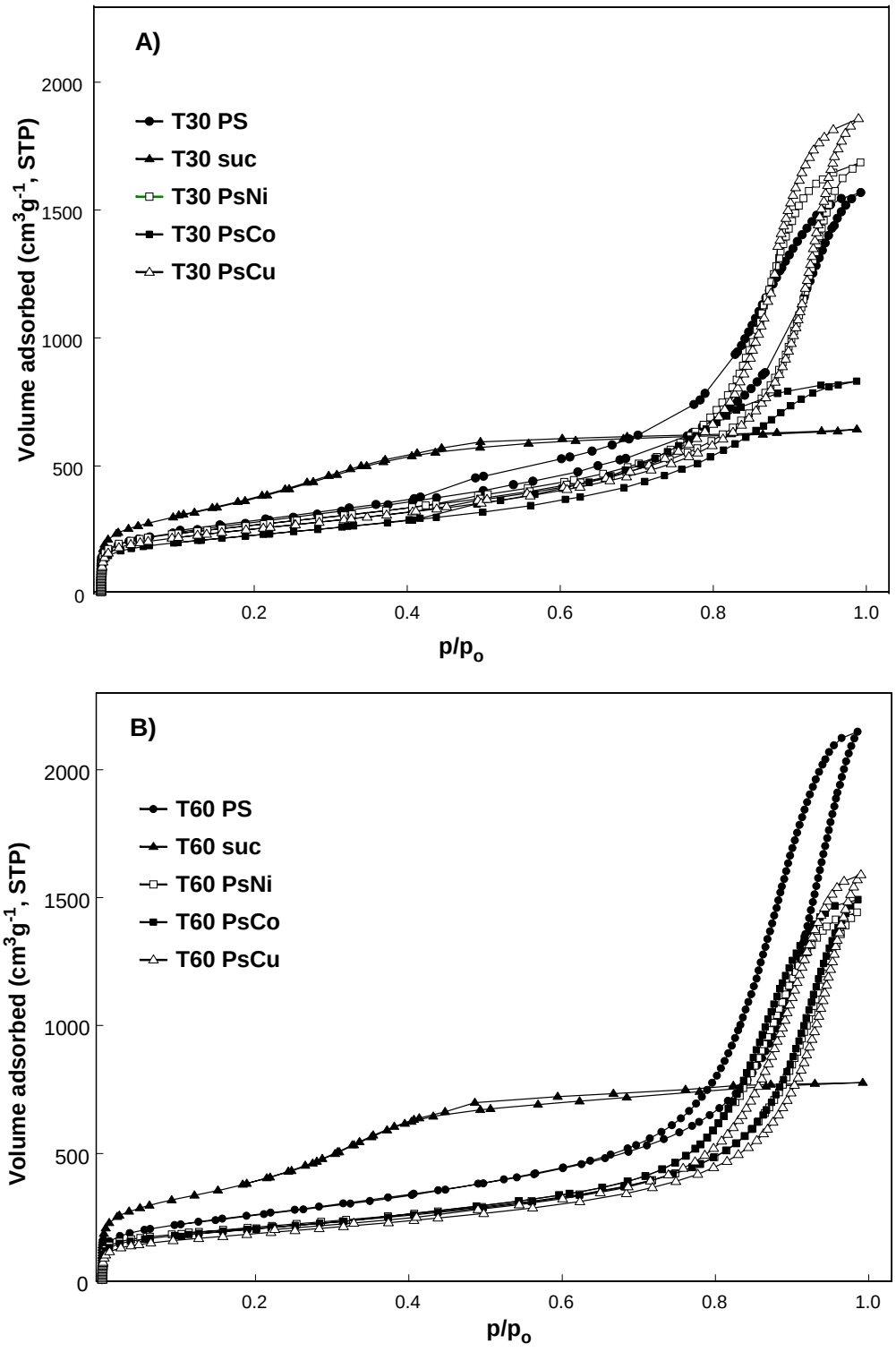

Fig. 8. Pore size distributions for carbons derived in T30(A) and T60 (B) silicas, obtained from nitrogen adsorption data